

# A Method for Determining SF6 Circuit Breakers Failure Rate Due to Transient Recovery Voltage

Reza Ghanizadeh<sup>1\*</sup>, Allahverdi Azadrou<sup>2</sup>

<sup>1</sup>Department of Electrical Engineering, Urmia Branch, Islamic Azad University, Urmia, Iran

<sup>2</sup>Department of Electrical Engineering, Salmas Branch, Islamic Azad University, Salmas, Iran

Email: r.ghanizadeh@iaurmia.ac.ir(Corresponding author) , [azadrou.elec@gmail.com](mailto:azadrou.elec@gmail.com)

Receive Date: 10 March 2022, Revise Date: 15 April 2022, Accept Date: 10 June 2022

**Abstract:** *In this paper, a method is presented for determining SF6 Circuit Breakers (CBs) failure rate due to Transient Recovery Voltage (TRV) at the instant of interrupting short-circuit current. For this purpose, first, discharging of electric charge due to arcing, which is the main cause of erosion in CB contacts, is calculated using transient state simulation of EMTP/ATP software. This arcing takes place due to interruption of short-circuit current by the CB. Since the location of short-circuit on the line is unknown, a statistical approach is presented for determining its location. Accordingly, the statistical distribution of short-circuit location is formed based on the data recorded at 110kV Tatev station. Based on this statistical distribution, the CB failure is detected using the arcing contact wipe index ( $D_a$ ). Finally, the CB failure rate is obtained based on the number of failures during 100 times of fault clearing. Compared to the previous works, simulation results show the accuracy of the proposed method and proper performance of the CBs used for supplying the 110kV Transmission Lines (TLs).*

**Keywords:** SF6 circuit breaker, failure rate, short-circuit current, transient recovery voltage, arcing contact wipe.

## Nomenclature

TL	transmission line		distribution of short-circuit
CB	circuit breaker	$X_1, X_2$	two samples of random short circuit location
TRV	transient recovery voltage		
$D_a$	arcing contact wipe	$u_n$	distributed random numbers
$\Delta U_{eff}$	effective slope voltage	$n$	number of current interruptions
$C$	line capacitance	$\rho$	density of the contact material
$I_0$	initial current in line inductance	$A_n$	cross section area of the contact
$t_{open}$	instant when CB contacts open	$m_n$	loss of contact material mass
$t_{interrupt}$	instant of current interruption	$h_{vap}$	enthalpy of the contact material
$i(t)$	current passing through the arcing path	$t_{arc,n}$	instant of arc occurrence
$Q_{discharged}$	discharged electric charge		
$\mu, \sigma$	mean and standard deviation of normal		

## 1. Introduction

A major portion of electric power in power systems is transmitted through Transmission Lines (TLs). Therefore, in order for the electrical energy to flow

continually, protection of TLs is of great importance [1]. In addition to insulation breakdown of line isolators, failure of Circuit Breaker (CB) in the station is one of the reasons of failure in TLs [2]. Therefore, the CB needs to be studied from transient

state perspective, its failure rate must be calculated and proper insulation coordination has to be adopted to prevent its failure.

A CB is an automatic switch that is capable of turning the current on and off under nominal conditions. Furthermore, a CB is able to interrupt the current under short circuit conditions. To provide stability and reliability in power network, the CB must be able to interrupt the short-circuit current. Contacts of a CB are closed under nominal conditions and current flows through them [3]. Upon receiving a tripping signal, CB contacts are opened. In practical CBs, when the contacts are being separated, an electric arc is created and the CB is changed from conductor to insulator. Interrupting the current of a resistive load does not cause any problem. Because in this case, when the CB interrupts the current, the voltage across its contacts increases from zero and gradually reaches its peak value (according to the power frequency voltage), and this continues until the contacts are fully opened. However, power TLs often have inductive loads, and opening the contacts is accompanied by a significant increase in the voltage across CB contacts, which continues until reaching the TRV value [4]. This value of voltage is greater than the nominal peak voltage; therefore, under such conditions, it is likely that arcing continues even through open contacts, and CB contacts are destroyed. The closer the location of short circuit to the station, the lower the short circuit impedance and the more intense the short circuit current. Short circuit currents with higher amplitude impose higher electric charge to the CB contacts through arc path and cause

more erosion. Basically, the location of short circuit in TL is unknown; therefore, a CB failure is a non-deterministic phenomenon. Accordingly, to investigate the CB failure rate, it is necessary to determine the number of times that the CB has not been able to isolate the short circuit from the station due to high erosion of its contacts.

So far, only a small number of studies have been conducted on CB failure rate, and most of these studies are related to the CB contacts erosion and limited to experiments performed in laboratories. These experiments have been carried out with the objective of determining a procedure for periodic tests of high voltage CBs. Based on accurate studies, authors in [5] have investigated CB test methods and presented accurate statistics using field tests. According to this reference, to consider the reconfiguration changes over the 25-year lifespan of a CB, a convention has been set up in order to establish a balance between generation and consumption. Reconfiguration causes the short-circuit current to increase; therefore, the amplitude of the current that the CB needs to be able to interrupt increases as well. Consequently, the CB must be selected in a way that future load expansion planning is taken into consideration. According to this convention, the CB must be able to operate with its full capacity over 30 percent of its lifespan, and over the remaining 70 percent, it must be able to operate with 70 percent of cut-off capacity. In other words, the CB capacity needs to be selected in a way that the last 30% of the CB lifespan is concurrent with load expansion in which the short circuit capacity is not greater than the CB interruption

capacity. This convention guarantees that the CB will show a proper performance at interrupting short-circuit currents over its 25-year lifespan. In [3], the process of arc forming has been discussed in details and TRV has been explained based on analytical relations and physical principles of arc forming. In [4], in addition to describing the details of TRV model, their equivalent circuit and analytical equations have been explained. In [6], using experimental approaches, effective slope voltage ( $\Delta U_{eff}$ ) has been presented for SF6 CBs with different contact materials. In [7], by simulating an experimental case, a criterion has been presented for determining CB maintenance cycle. Although this criterion has been presented for determining the amount of erosion in CB contacts in order to determine their maintenance time, it is suitable for experimental test conditions with low short-circuit current, and it has no practical application in real-world networks. In [2, 8-12], probabilistic investigation of power network problems has been carried out. In [2], a risk criterion has been introduced for investigating power network and TLs in order to properly design the network insulation. In [9-10], the authors have addressed the network insulation coordination against overvoltage due to lightning and switching, which are among the main reasons of short circuit in the network.

In this paper, a method is presented for determining the failure rate of SF6 CBs due to TRV. Accordingly, for actual operating conditions in the station, first the amount of electric charge, which is discharged due to

arcing, is calculated. This arc is generated because of occurrence of a random short circuit at a point of TL. Statistical distribution of short circuit location is provided based on the data recorded in Tatev station, which supplies a 110kV TL. According to this statistical distribution, the CB failure is detected using  $D_a$ . Finally, the CB failure rate is obtained based on the number of times that the CB encounters failure over 100 times of fault clearing. The most important contributions of this paper are as follows:

- Estimating the CB failure rate due to interrupting the short circuit current.
- Presenting a novel method for CB erosion using a statistical approach.
- Estimating the location of potential short circuits using statistics obtained from feeding station.
- Presenting a new method to estimate the effect of short circuit location and short circuit current on CB erosion.

## 2. Transient state of CB opening

The transient voltage across the CB shown in Fig. 1a is used to interrupt the inductive load current shown in Fig. 1b. Although this circuit is more complicated in practical systems, this case shows that interrupting the current of inductive loads is more difficult than resistive loads. In addition, switching inductive loads may generate severe high frequency TRV, which is related to the fast interruption of the current and is known as arc chopping. A brief discussion about the process of interrupting inductive load current is presented below. If the current is interrupted at zero-crossing point of the

current cycle, TRV will be within the allowed range [2]. However, if a premature interruption occurs, the process of interruption will be abnormal due to stresses caused by the short-circuit current, and this will result in generation of high frequency arcs and overvoltage. When the CB stops the peak current, its voltage increases instantaneously; if this overvoltage exceeds insulation strength of the CB, arcing takes place again [3]. When this process is repeated for several times, due to fast arcing, the voltage increases rapidly and leads to high frequency fluctuations in the voltage. These high frequency fluctuations depend on the electrical parameters, arrangement of the circuit and the process of interrupting the current. If a capacitor is used to model the line stray capacitance, when the CB opens, electrical energy is exchanged between the magnetic field of line inductance and electric field of line capacitance according to the following equation:

$$f = \frac{1}{2\pi\sqrt{LC}} \quad (1)$$

The maximum generated voltage is equal to [3]:

$$V_{\max(pu)} \approx \sqrt{1 + \frac{L}{C}} I_0^2 \quad (2)$$

where,  $C$  is the line capacitance and  $I_0$  is the initial current stored in the line inductance.

By calculating the discharged electric charge, the stress of TRV on the CB at the instant of interruption of short-circuit current can be determined. The factor that causes CB erosion at the instant of short-circuit current interruption is the electric charge discharged due to arcing. The electric charge discharged

at CB can be calculated using the following equation:

$$Q_{\text{discharged}} = \int_{t_{\text{open}}}^{t_{\text{interrupt}}} i(t) dt \quad (3)$$

where,  $t_{\text{open}}$  is the instant when CB contacts open,  $t_{\text{interrupt}}$  is the instant of current interruption, and  $i(t)$  is the current passing through the arcing path which will be obtained by transient state simulation of EMTP/ATP.

To carry out transient state simulation of EMTP, the short-circuit location on the line needs to be known. Basically, the location of short circuit on the line is not known. Therefore, in this paper, a statistical approach is presented for determining the short-circuit location. Accordingly, having formed the statistical distribution of short-circuit location using the recorded data, and having extracted the mean and standard deviation values using the congruential method, the random location of the next short-circuit can be determined by means of the random location of the previous short circuit, as shown by the following equations [13]:

$$x_n = (c \cdot x_{n-1} + b) \cdot \text{mod}(m) \quad (4)$$

$$u_n = \frac{x_n}{m} \quad (5)$$

$$X_1 = \mu + \sigma(-2 \ln u_1)^{0.5} \cos(2\pi u_2) \quad (6)$$

$$X_2 = \mu + \sigma(-2 \ln u_1)^{0.5} \sin(2\pi u_2) \quad (7)$$

where,  $b$ ,  $c$ , and  $m$  are positive integers that are equal to 150889, 1366 and 714025, respectively;  $u_n$  is a set of random numbers distributed between 0 and 1. Parameters  $\mu$  and  $\sigma$  are, respectively, the mean and

standard deviation of the normal distribution of short circuit;  $X_1$  and  $X_2$  are two extracted samples of random short-circuit location, which are in conformity with the distribution.

## 2. CB Erosion

To increase the reliability and stability of power networks, CBs must be able to interrupt the short-circuit current. Interrupting short-circuit currents causes erosion in CB contacts. If the erosion is too severe, the CB must be repaired before being operated again. One of the best ways to investigate the amount of erosion is to periodically disassemble CBs, and this has its own maintenance and power failure costs. In this paper, a method is presented which can be used to notify about the erosion by using arcing contact wipe ( $D_a$ ) without needing to disassemble the CB.

As shown in Fig. 2, parameter  $D_a$  consists of two parts; i.e.,  $D_{sc}$  and  $D_{usc}$ ;  $D_{sc}$  clearly decreases with the increment in number of interruptions of short-circuit current, while  $D_{usc}$  remains almost unchanged. Therefore, the ratio  $D_{sc}/D_{usc}$  increases [14]. It is assumed that erosion in CB takes place due to evaporation of contact materials and  $D_a$  losses occur only on fixed contacts [15]. Therefore,  $D_a$  for n-th ( $D_{a,n}$ ) short-circuit current can be calculated using the following equation:

$$D_{a,n} = D_{a,n-1} - \Delta D_a = D_{a,n-1} - \frac{m_n}{\rho A_n}, \quad n=1,2,3,\dots \quad (8)$$

where,  $n$  is the number of current interruptions,  $\rho$  is the density of the contact material,  $A_n$  is the cross section area of the contact in which heat conduction takes place

and  $m_n$  is the loss of contact material mass, which can be calculated using the following equation [8]:

$$m_n \approx \frac{\Delta U_{eff} \cdot Q_n}{h_{vap}} - \frac{2 \cdot C_{cb} \cdot A_n \sqrt{t_{arc,n}}}{h_{vap}} \quad (9)$$

where,  $\Delta U_{eff}$  is the effective slope voltage,  $h_{vap}$  is the enthalpy of the contact material from 20<sup>0</sup>c to the evaporation temperature and  $t_{arc,n}$  is the arcing instant [7]. Since TRV is a complicated phenomenon, to take it into account, it is necessary to simulate the transient state of CB opening; this paper obtains  $i_n(t)$  and  $t_{arc,n}$  from simulation of EMTP during separation of short-circuit from the line. If  $D_a$  is less than its critical value ( $D_a < 2.19$ ), the CB must be repaired.

## 3. TL Under Study

Geographical location of the line under study, which is between Tatev and Kajaran stations, is shown in Fig. 3. The length and voltage level of this line are 80km and 110kV, respectively. Switching statistics of the CB in the line under study over its 25-year lifespan is presented in Table 1. According to this table, it can be concluded that the short-circuit caused by the lightning was due to the surge arrester failure. Based on the isochronic curve, the probability of being stricken by lightning is the same for all points along the entire line. In addition, the failure caused by switching overvoltage in the middle of the line is due to the shift of maximum overvoltage to the middle of the line because of installation of lightning arresters on both ends of the line.

#### 4. Simulation Results

In Fig. 4a, the simulation of the line under study in EMTP/ATPDraw software is shown. The length of TL is 80km and its nominal voltage is equal to 110kV at 50Hz. The total length of the line is divided to 8km long sections and the same line model is used for each section. The value of the impedance behind the source is given in Table 2. The configuration of the tower and conductors of the line under study is shown in Fig. 4b. Moreover, data of the SF6 CB used in simulations is presented in Table 3. In modeling multi-phase long TLs, lumped models of line are not used, since they are inaccurate. One of the models, which are usually used, is the  $\pi$  model. Variations of line parameters such as resistance, inductance and capacitance are functions of frequency, which is assumed to be fixed in this model. In this paper, in order to study short circuit transient states, the frequency dependent JMarti model is used. This model takes the variations of line parameters into account as functions of frequency because the transient waves in power systems contain a wide range of frequencies [16]. In JMarti model, in addition to the configuration of line and nominal frequency, the minimum and maximum value of frequency under study need to be determined.

The process of interrupting the short-circuit current occurred in phase “a” 40km farther from the supplying station is shown in Fig. 5. After occurrence of a short circuit, it takes 50ms for the fault current to disappear. At the last ten seconds while the CB contracts are unlatched, due to the TRV

phenomenon, the voltage across CB is greater than the insulation strength of anti-arcing material between them, and a closed path is provided through the arc path. This process, during which the distance between CB contacts increases sufficiently to overcome the TRV across the CB, continues until the moment that short-circuit current cycle crosses zero, and the contacts are sufficiently far from each other. Therefore, the electric charge discharged at the CB due to arcing causes erosion in contacts. Resulting from the simulations performed in EMTP/ATP software, Fig. 6 shows the process of interrupting short-circuit current in the network under study for short circuits that take place at distances of 8 and 80km from the supplying station at 0.0285 sec for which the breaker opens at 0.075 sec. It is clear that the closer the short-circuit location to the supplying station, the more severe the short circuit, and the higher the amount of electric charge discharged at CB.

Fig. 7 shows the amount of electric charge discharged due to arcing for the short circuits shown in Fig. 6 between 0.075 and 0.085 sec. According to Fig. 5, although the currents of unfaulted phases are slightly distorted, they are symmetric. Therefore, the current of the faulted phase is substituted in Equation (3), and the electrical load is calculated according to Fig. 7. As can be seen in Fig. 7, as the short-circuit location gets closer to the station, the discharging of electric charge at CB through the arcing path is more severe.

Using data clustering approaches, the data related to the location of short-circuit on the line under study are fitted in such a way that

the normal statistical distribution of the short-circuit location for the line under study is as shown in Fig. 8. The values of  $\mu$  and  $\sigma$  of the distance between the short-circuit location and the station are obtained to be 42 and 8 km, respectively. These data are based on Table 1 and the statistics are presented by Tatev station. According to this figure, the short-circuits have usually occurred at the end points of the lines, and the reason behind this is more severe overvoltage resulted from switching and lightning.

As shown in Fig. 9, locations of 35 future short-circuits are extracted by using the normal distribution of Fig. 8 and Equations (9) to (11). The amount of electrical load discharged through arcing path is calculated by simulation of transient state as shown in Fig. 7. Each time after the CB clears the fault from the line, the amount of erosion in contacts,  $D_a$ , is obtained using Equation (8). If the value of  $D_a$  is less than the critical value of 2.19 mm [7], the contacts must be inspected and replaced. In Fig. 10, the value of  $D_a$  is shown after each separation of short-circuit. Five bars in the diagram, represent 5 times of contact replacement. Thus, after 7 times of short-circuit separation, the contact is replaced, and the diagram goes on from the next row. As can be seen in Fig. 10, the amount of decrement of  $D_a$  is minimum for the cases in which the fault has occurred at the end of the line. This is because the short-circuit is mild and the electric charge discharged through arcing is small. It is worth noting that if the value obtained for  $D_a$  is less than the threshold value of 2.19 mm, the CB needs to be removed from the circuit and repaired.

## 5. CB Failure Rate

The failure rate of the CB can be calculated after occurrence of 100 short-circuits, the location of which can be determined based on Equations (9-11). According to Equation (8), the failure of a CB takes place when  $D_{an} < 2.19$ . Moreover, it is assumed that the CB contacts are inspected after 5 times of short-circuit separation. Therefore, the failure rate of CB, i.e., the probability that  $D_a$  is less than 2.19 ( $P(D_{an} < 2.19)$ ), is expressed as follows:

$$D_{a0} - D_{a1} - D_{a2} - D_{a3} - D_{a4} < 2.19 \quad (10)$$

Considering an initial value of 14mm for  $D_{a0}$ :

$$D_{a1} + D_{a2} + D_{a3} + D_{a4} > 11.81 \quad (11)$$

To calculate the probabilistic Equation (11), according to statistical distribution of Fig. 8, variations of arcing contact wipe, shown in Equation (8), are calculated for 100 times of short-circuit occurrence and the result is shown in Fig. 11. Therefore, after each separation,  $D_a$  is calculated. On the other hand, after 5 short-circuits, the CB is removed and inspected. Before the inspection time is reached, if  $D_a$  is so eroded that it cannot completely absorb the electric charge of the arc in the next short-circuit, the circuit breaker will be destroyed. As shown in Fig. 11, only in 7 cases, the variations of  $D_a$  exceed the threshold value of Equation (11); therefore, the failure rate will be 7%. This means that only in 7 out of 100 times of short-circuit fault clearing, the short-circuit location is close to the station, and considering the predefined 25-year lifespan for each circuit breaker, occurrence of 100 times of separation will last 60 years [6].

Therefore, line failure risk due to the failure of interrupting CB in the station is equal to:

$$CB. Failure Risk = 7 \times \frac{25}{60} = 2.9\%$$

Consequently, according to the approach presented in this paper, the outage risk is insignificant.

## 6. Comparison with Previous Studies

To show the efficiency of the proposed approach, the simulation results are compared with [7]. In this reference, the index  $N_{100\%}$  is used to calculate the amount of erosion in contacts.

$$\begin{cases} N_{100} = -1.89D_a + 26.51 \\ N_{100\%} = \frac{N_{100}}{N_{100,r}} \end{cases} \quad (12)$$

where,  $N_{100,r}$  is the number of allowed short-circuit interrupting operations. If  $N_{100\%} < 35$ , the contact has no problem, and according to [7], if  $35 < N_{100\%} < 70$  the contact needs to be inspected, and if  $N_{100\%} > 70$ , the contact is at risk. Table 4 shows the values of circuit breaker risk ( $N_{100\%}$ ) for different cases.

According to [7], during laboratory tests of CB, it is necessary to repair and replace the CB as soon as  $N_{100\%}$  exceeds 70%; however, according to the results presented in Table 4, since the stress due to arcing is high, the value of  $N_{100\%}$  has been 32.82% the last time that the CB could have been utilized. In Table 4, the borders of the cells in which  $N_{100\%}$  exceeds 30% are drawn in bold (the cell borders drawn in bold to represent the boundary beyond which  $N_{100\%}$  exceeds 30%). According to [7], the

threshold value of 30% is introduced so that more attention is paid to the CB. In Table 4, the cases in which the CB will encounter problems after clearing the fault are highlighted. Therefore, this paper proposes to remove the CB for inspecting the contacts after 5 times of short-circuit separation. In this method, based on the simulations in Fig. 10, after the third CB maintenance operation and during the fourth short-circuit clearing operation, the state of contacts becomes critical; however, the method presented in this paper prevents CB failure. It is worth noting that if the fault location is close to the station, the proposed method will not be fully effective; however, such cases are rare, and as a result, premature removing of CB will be prevented.

## Conclusion

In this paper, using the CB erosion index, a new statistical method was presented to investigate the failure rate of SF6 CBs. This method is based on the short-circuit data recorded at 110kV Tatev station. Accordingly, first the line under study was implemented in EMTP/ATP software, and the amount of electric charge discharged during CB opening was calculated. Then, according to the amount of load discharged, the amount of erosion in CB contacts was obtained using  $D_a$ . Finally, the CB failure rate was obtained based on the number of failures over 100 times of fault clearing. Therefore, the accurate value of failure rate over the course of CB lifespan can be obtained using the proposed method. This can be a measure for line insulation designers to decrease failures of TLs.



## References

- [1] IEC/TR 62271-310. High-voltage switchgear and control gear — part 310: electrical endurance testing for circuit-breakers above a rated voltage of 52 kV 2008; 2nd edition.
- [2] Hileman A. R. Insulation coordination for power systems. Marcel Dekker Inc., New York, 1999.
- [3] Martinez-Velasco J. A. Power System Transients Parameter Determination. Taylor & Francis Group 2010.
- [4] Smeets R, Sluis L. der, Kapetanovic M, Peelo D. F, Janssen A. Switching in Electrical Transmission and Distribution Systems. John Wiley & Sons 2015.
- [5] Pons A, Sabot A, Babusci G. Electrical endurance and reliability of circuit-breakers common experience and practice of two utilities. IEEE Transactions on Power Delivery 1993; 8(1): 168-174.
- [6] Yokomizu Y, Matsumura T, Henmi R, Kito Y. Total voltage drops in electrode fall regions of SF6, argon and air arcs in current range from 10 to 20000 A. Journal of Physics D: Applied Physics 1996; 5(29): 1260–1267.
- [7] Chenga T, Gaoa W, Liua W, Li R. Evaluation method of contact erosion for high voltage SF6 circuit breakers using dynamic contact resistance measurement. Electric Power Systems Research 2018; 163: 725-732.
- [8] Shariatinasab R, Ghayur safar J, Akafi-Mobarakeh M. Development of an adaptive neural-fuzzy inference system based meta-model for estimating lightning related failures in polluted environments. IET Science, Measurement & Technology 2014; 8(4):187–195.
- [9] Shariatinasab R, Akafi-Mobarakeh M. Estimation of switching overvoltages on transmission lines using Neuro-Fuzzy method. Intelligent Systems in Electrical Engineering 2011; 2(3): 55-66.
- [10] Chmielewski T, Oramus P, M. Szewczyk M, Kuczek T, Piasecki W. Circuit breaker models for simulations of short-circuit current breaking and slow-front overvoltages in HV systems. Electric Power Systems Research 2017; 143: 174-181.
- [11] Glushkov D. A, Khalyasmaa A. I, Dmitriev S. A, Kokin S. E. Electrical Strength Analysis of SF6 Gas Circuit Breaker Element. AASRI Conference on Power and Energy Systems 2013; 57-61.
- [12] Zhanga X, Gockenbacha E, Liub Z, Chenc H, Yangc L. Reliability estimation of high voltage SF6 circuit breakers by statistical analysis on the basis of the field data. Electric Power Systems Research 2013; 103: 105-113.
- [13] Gonos I. F, Ekonomou L, Topalis F. V, Stathopoulos I. A. Probability of back flashover in transmission lines due to lightning strokes using Monte-carlo simulation. International Journal of Electrical Power & Energy Systems 2003; 25(3): 107-111.
- [14] Landry M, Mercier A, Ouellet G, et al. A new measurement method of the dynamic contact resistance of HV circuit breakers. IEEE/PES Transmission & Distribution Conference and Exposition: Latin America 2006.
- [15] Tepper J, Seeger M, Votteler T, et al. Investigation on erosion of Cu/W contacts in high-voltage circuit breakers. IEEE Transactions on Components and Packaging Technologies 2006; 29(3): 658–665.
- [16] ATPDraw Manual. ATPDraw for Windows version 3.5, Preliminary Release No. 1.1 2002.

Table 1. Switching statistics of CB of the line between Tatev and Kajaran stations for clearing short-circuit faults over 25 years.

Operation over 25 years \ Distance from station	0	8	16	24	32	40	48	56	64	72	80	Total number
	Clearing short-circuit	1	1	2	1	1	1	3	5	10	12	
Short-circuit due to overvoltage caused by load	0	0	0	0	0	0	1	1	2	4	5	16
Short-circuit due to overvoltage caused by line energization	0	0	1	1	0	1	0	2	5	7	15	32
Short-circuit due to overvoltage caused by lightning	1	1	1	0	1	0	2	2	3	1	3	15

Table 2. Data of behind source impedance of TL under study.

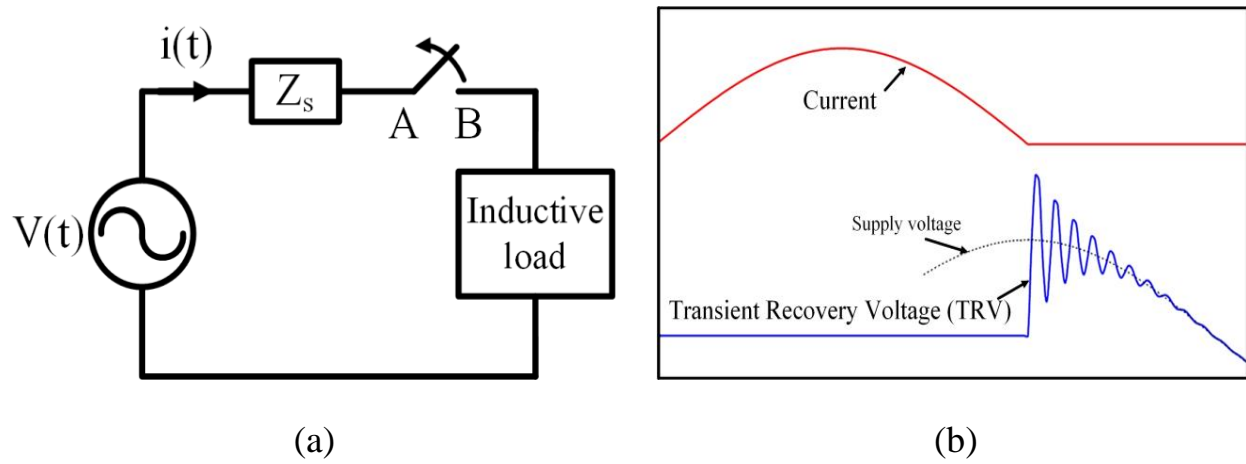
Parameters	Values ( $\Omega$ )
$R_0$	5.78
$X_0$	43.94
$R_+$	2.16
$X_+$	44.96

Table 3. Characteristics of SF6 CB used in simulation.

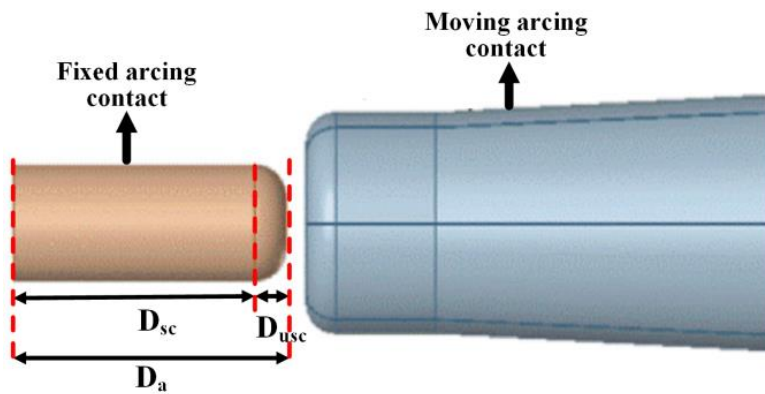
Parameters	Values
$\rho$	$1.515 \times 10^3 \text{ kg/mm}^3$
$A_n$	$2.545 \times 10^{-4} \text{ m}^2$
$\Delta U_{eff}$	21 (V)
$h_{vap}$	$4.6 \times 10^6 \text{ j/kg}$

Table 4. Value of  $N_{100\%}$  related to the number of clearing short-circuit faults over the maintenance period during the entire 25-year lifespan of CB.

Number of cleared short-circuit faults \ Period of maintenance	After CB installation	1	2	3	4	5
	1	4.89	1.56	6.07	4.45	6.90
2	9.27	5.94	7.57	9.27	13.57	8.4
3	18.75	10.32	11.59	13.65	20.59	12.78
4	23.57	18.27	16.33	18.48	32.43	20.73
5	25.07	22.65	20.72	24.48	-	22.22
6	33.01	27.47	25.54	25.98	-	28.23
7	-	28.97	32.38	32.82	-	-



**Fig. 1.** (a) simple circuit designed to interrupt inductive load current. (b) transient recovery voltage.



**Fig. 2.** Structure of breaker contact

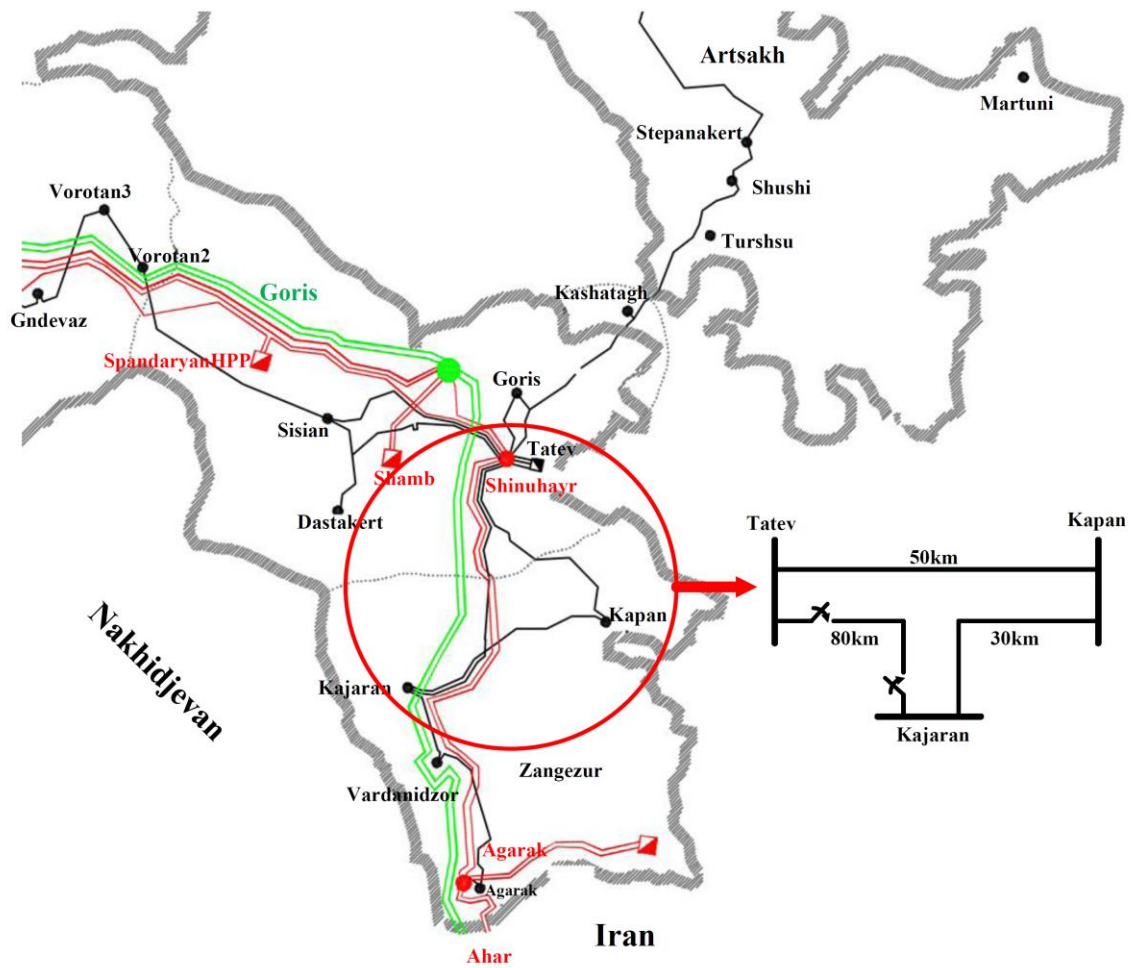
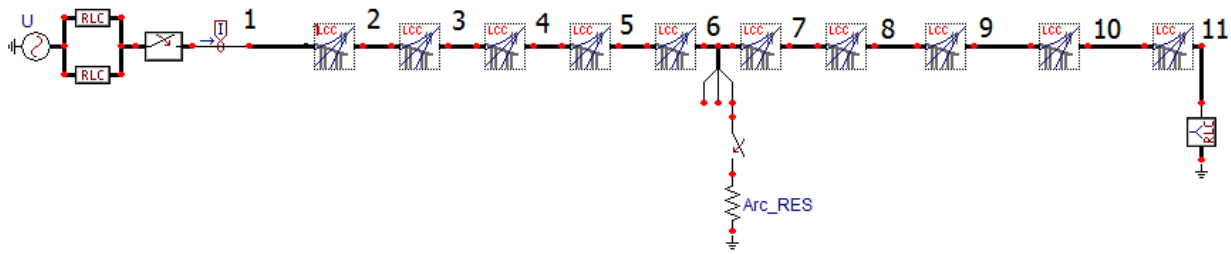
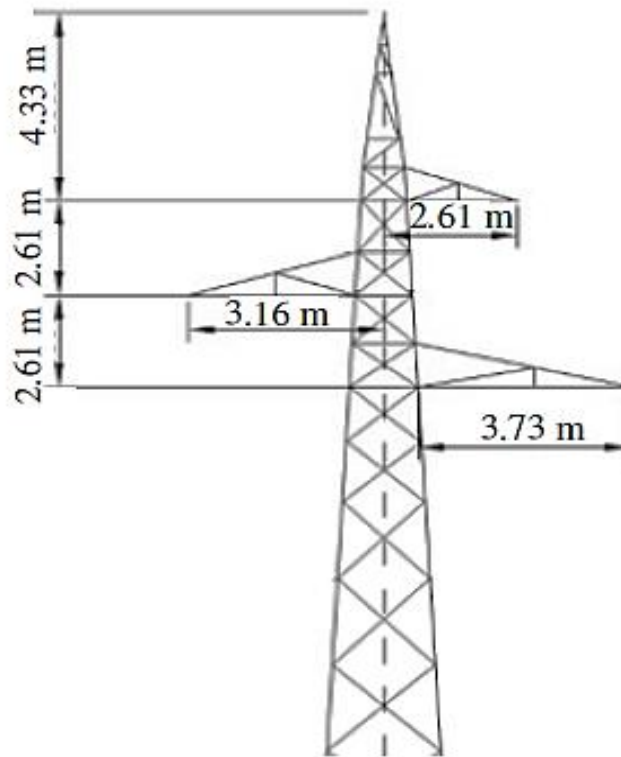


**Fig. 3.** Geographical location of TL under study (TL between Tatev and Kajaran stations).



(a)



(b)

**Fig. 4.** (a) 110 kV TL under study in EMTP/ATP software along with the short-circuit model at point 6 in a distance of 40 km from the station. (b) configuration of tower and conductors of TL under study.

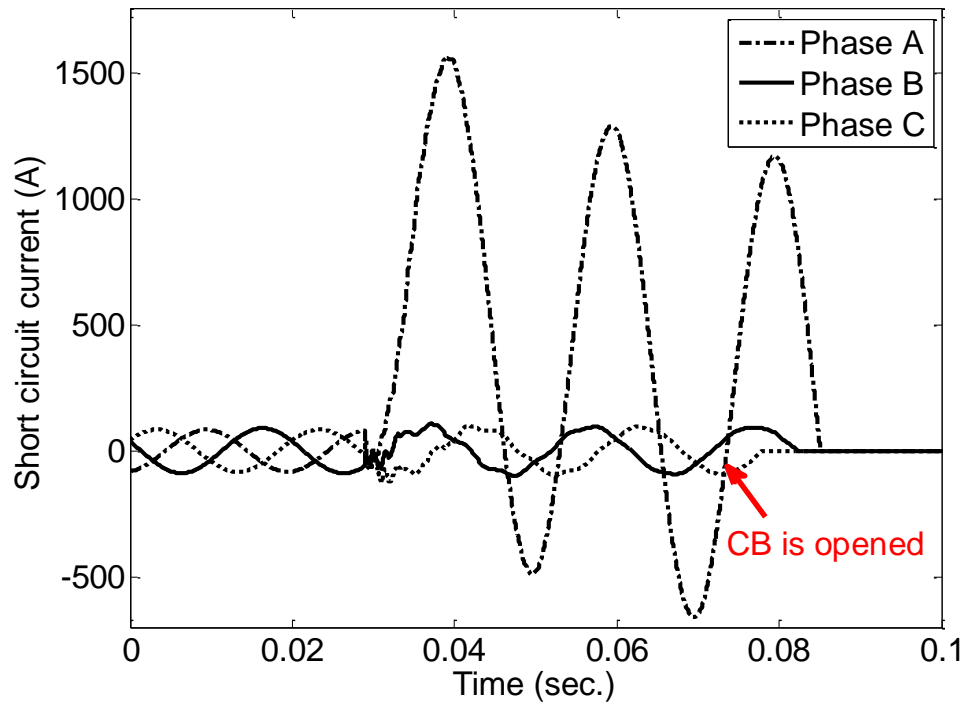


**Fig. 5:** A short-circuit taking place at  $t=0.0285$  sec at a distance of 40km from the supplying station and opening operation of CB at  $t=0.075$  sec.

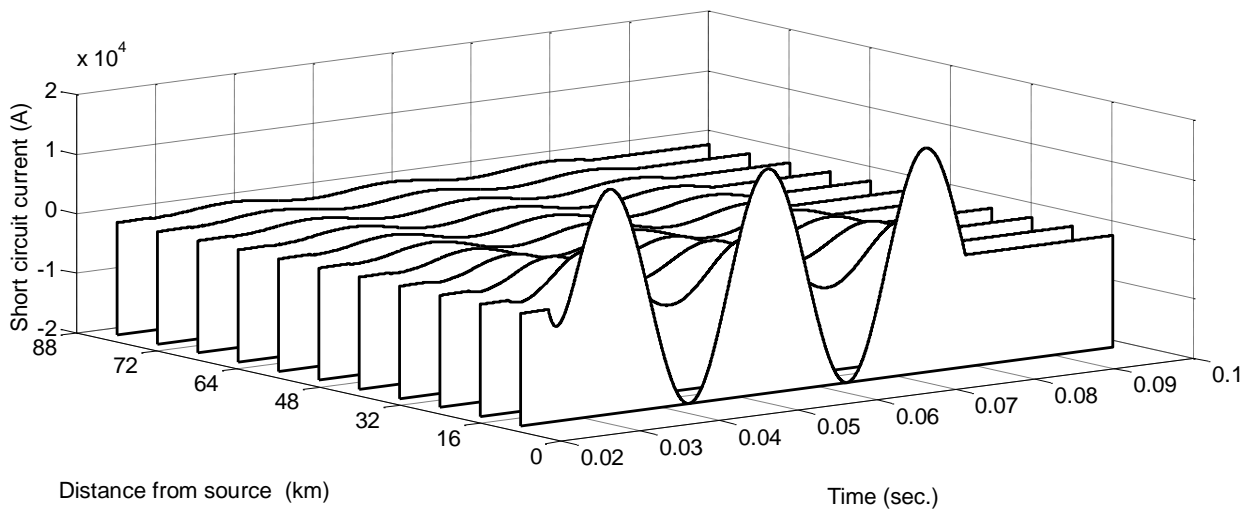


**Fig. 6:** A short-circuit taking place at distances of 0 and 80 km from the source and process of stopping it.

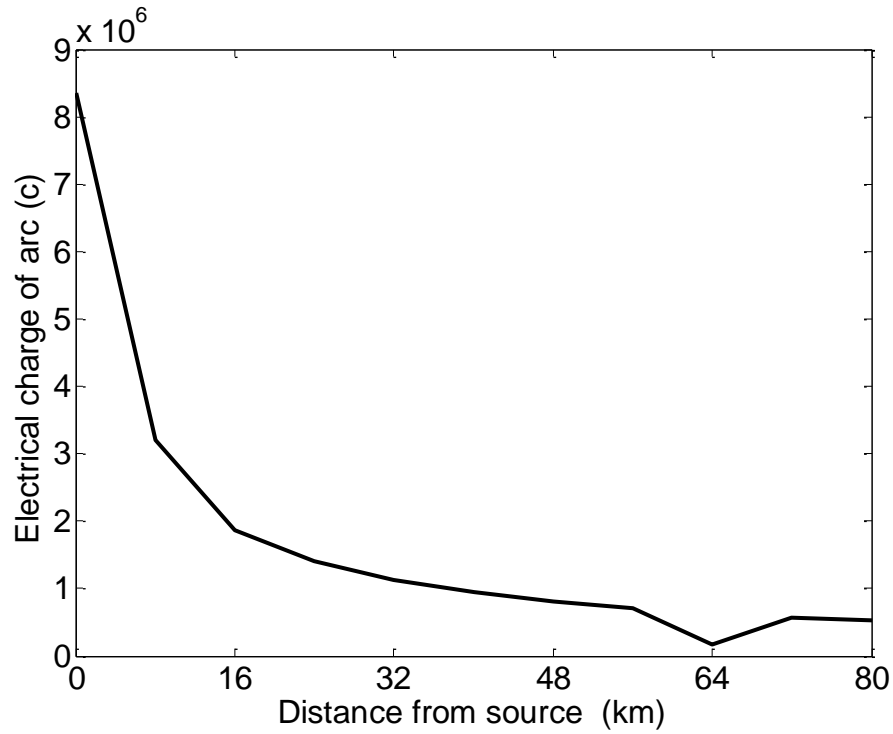


**Fig. 7.** Electrical load discharged at CB for a short-circuit taking place at a distance of 8 km from supplying station.

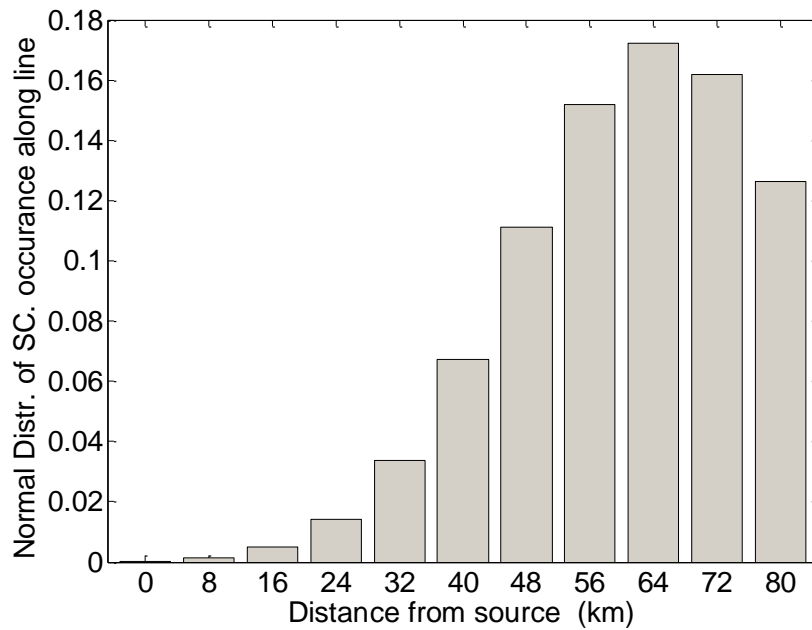


**Fig. 8.** Normal distribution of short-circuit occurrence along TL under study.

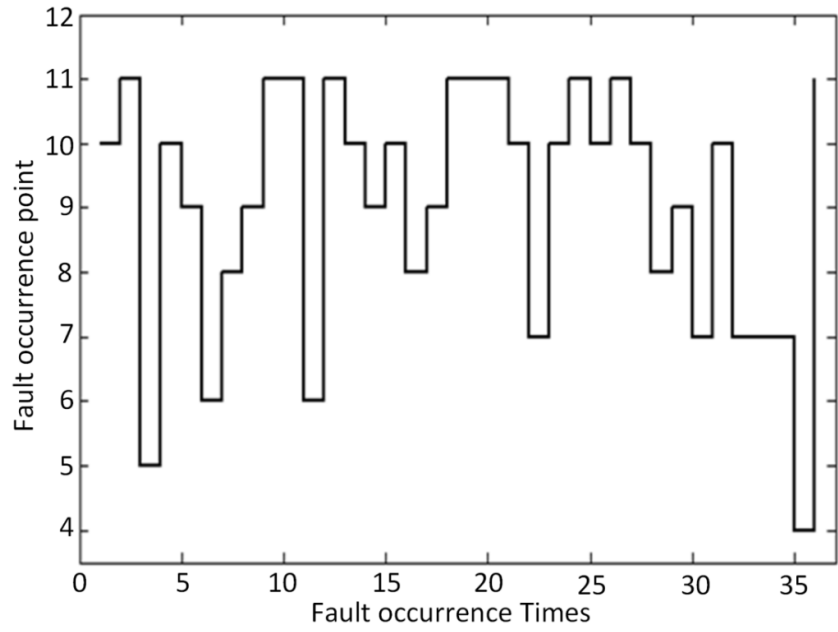


**Fig. 9.** Random fault occurrence locations in 35 future short-circuits.

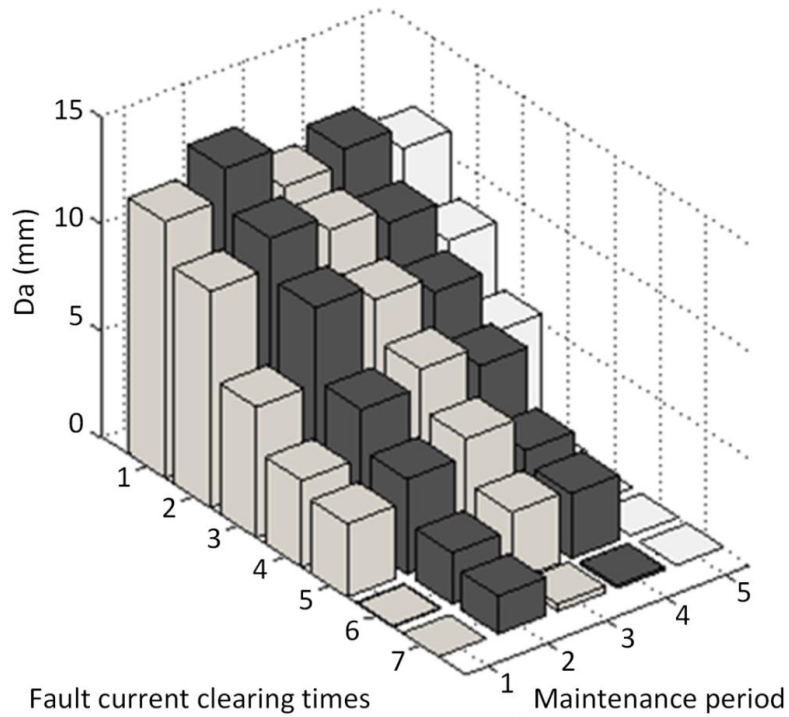


**Fig. 10.** Contact erosion versus the number of times that short-circuits faults are cleared during maintenance periods.



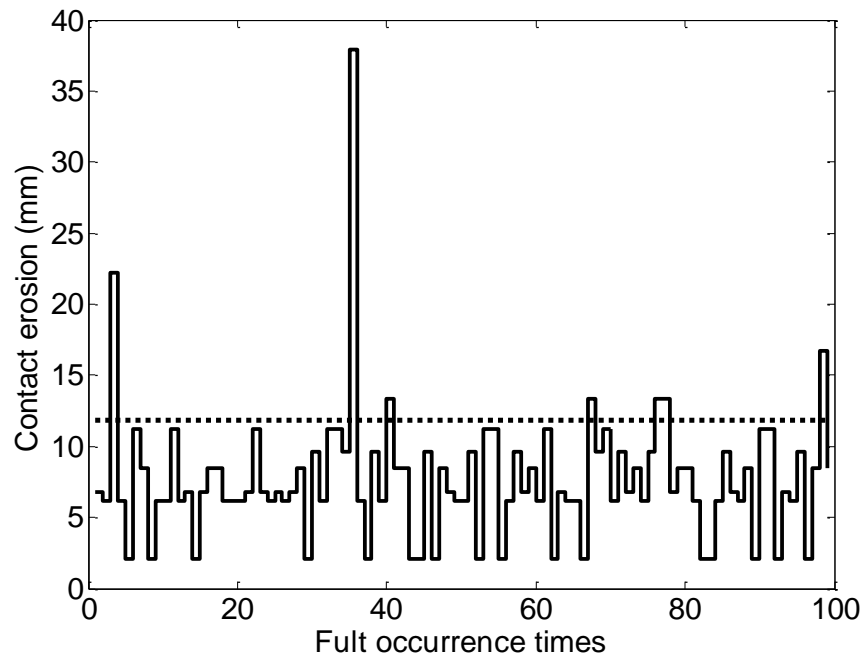


**Fig. 11.** Amount of erosion in CB contacts for 100 times of fault clearing considering normal distribution of the short-circuit occurrence.